C.H. Frazier and W.D. O'Brien, Jr. Image Formation with the Amplitude-steered Array using Time-frequency Distribution. *Acoustical Imaging*, 25, 535-542, 2000.

IMAGE FORMATION WITH THE AMPLITUDE-STEERED ARRAY USING TIME-FREQUENCY DISTRIBUTIONS

Catherine H. Frazier and William D. O'Brien, Jr.

Bioacoustics Research Laboratory
Department of Electrical and Computer Engineering
University of Illinois
405 N. Mathews Avenue
Urbana, IL 61801

INTRODUCTION

The amplitude-steered array, introduced by Hughes and Thompson in 1976 [1], was originally designed to steer a monochromatic signal to a particular direction. The array is now being considered for a fast imaging system [2]. The amplitude-steered array spatially separates frequencies in one direction, which allows a sector to be scanned with a single pulse. Images can be formed by calculating the spectrogram, which is the magnitude-squared of the short-time Fourier transform (STFT). The temporal position of the processing window gives information about the range of the target, and the frequencies contained within the window give information about the lateral position of the target. Although the spectrogram is conceptually simple and easy to program, there are several drawbacks that make it possibly undesirable as the means for forming the image. In particular, there is an inherent tradeoff between time and frequency resolution, so that an improvement in one implies a degradation in the other.

Many time-frequency distributions have been studied for various purposes, each having its own benefits and drawbacks. It is generally accepted that the best distribution for an application must be chosen based on the properties of the signal and the criteria for the result. We compare five distributions for a test signal, that is a simulated reflection from seven point targets. The distributions we have chosen are the spectrogram, the constant-Q spectrogram [3], the Wigner distribution [4], the smoothed pseudo-Wigner distribution [5], and the Choi-Williams distribution [6]. In sonar applications, time-frequency representations and time-frequency filtering have been used to identify targets [7], [8]. In our application, we do not identify targets based on characteristics of the distribution, but rather, we use the time-frequency distribution to form an image of the target.

In the next section, we describe how the amplitude-steered array is used to collect data. Then we discuss properties of each of the distributions. Next, we describe our test signal,

Acoustical Imaging, Volume 25, Edited by Halliwell and Wells.
Kluwer Academic/Plenum Publishers, 2000.

and the basis for comparison of each of the distributions. Finally, we give results and conclusions. In the following discussion, the terms time-resolution and frequency-resolution are used; however the terms range-resolution and lateral-resolution, respectively, could easily be substituted.

ARRAY FIELD PATTERN

The array pattern for an amplitude-steered array with an even number of elements can be written as [1],[2]

$$H(\theta) = \frac{2}{N}[\cos\phi\cos u + \cos 3\phi\cos 3u + \ldots + \cos((N-1)\phi)\cos((N-1)u)] \quad (1)$$
$$+\frac{2}{N}[\sin\phi\sin u + \sin 3\phi\sin 3u + \ldots + \sin((N-1)\phi)\sin((N-1)u)]$$

where θ is measured from the array broadside direction, N is the number of elements in the array, ϕ is a constant equal to $(k_0 d\sin\theta_0)/2$, and u is equal to $(kd\sin\theta)/2$. θ_0 is the design steering angle, k_0 is the wavenumber at which the beam will be steered to θ_0, and d is the interelement spacing. In Equation (1), $cos((2n-1)\phi)$ and $sin((2n-1)\phi)$ terms are constants which we interpret as amplitude weights on the elements. The beam is steered by weighting the elements. The $cos((2n-1)u)$ and $sin((2n-1)u)$ terms represent combinations of pairs of elements on opposite sides of the center of the array in-phase or 180° out of phase, respectively. Equation (1) can be interpreted as the sum of the outputs of two arrays.

If the array described above is excited by a frequency different from the design frequency used to calculate ϕ, the maximum response will occur at an angle different from the designed steering direction, θ_0.

$$\phi = \frac{k_0 d\sin\theta_0}{2} = \frac{k_f d\sin\theta_f}{2} \quad (2)$$

$$\theta_f = \sin^{-1}\left(\frac{f_0}{f}\sin\theta_0\right) \quad (3)$$

The subscript, f, was added to k and θ to emphasize that the new steering direction is calculated for a specific frequency, f.

An example of several beams from a 9.76-cm-length array is shown in Figure 1. The array is designed to steer to 5° at 5.6 MHz. Beams are shown for 5.6 MHz (5°), 4.5 MHz (6.23°), 3.4 MHz (8.25°), 2.3 MHz (12.25°), and 1.2 MHz (24°).

TIME-FREQUENCY PROCESSING FOR IMAGE FORMATION

In this section, we briefly describe the properties of the time-frequency distributions used to form images. Expressions are given for calculating only the discrete distributions. More detailed discussions and expressions for calculating the continuous distributions can be found in the references for the distributions provided in the introduction.

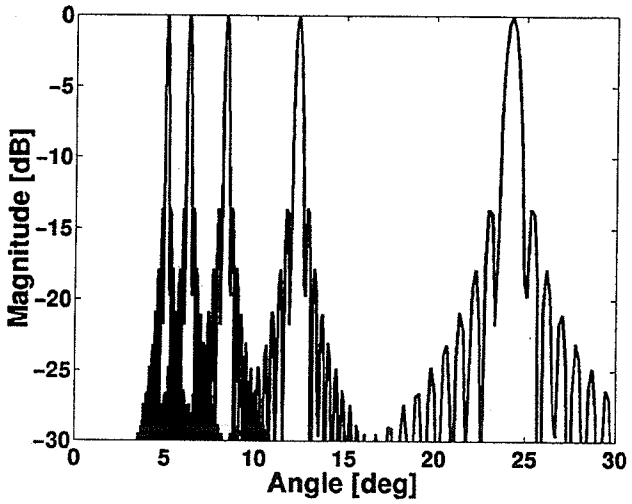

Figure 1. Beams from a 9.76-cm aperture steered to 5° at 5.6 MHz. Beams are shown for 5.6 MHz (5°), 4.5 MHz (6.23°), 3.4 MHz (8.25°), 2.3 MHz (12.25°), and 1.2 MHz (24°).

Spectrogram

The spectrogram, which is the magnitude-squared of the STFT, is the classic method for studying signals whose spectra vary with time. The spectrogram has the advantage that oscillating cross-terms, which are present for some distributions, are reduced to zero as long as the signal components do not overlap in time. And the spectrogram is a nonnegative definite distribution which leads to easy interpretation as an image.

The time and frequency resolution of the spectrogram are determined by the length of the window used in the calculation. Different tradeoffs can be made by changing the window shape. However, the window cannot be narrow in both the time and frequency domain, so there is an inherent tradeoff in resolution for the spectrogram.

Constant-Q Spectrogram

The constant-Q distribution is a special case of the spectrogram, where the window length is chosen based on the frequency sample being calculated. The number of cycles in the window is kept constant; therefore, a constant ratio between center frequency and bandwidth, can be maintained.

The expression for the constant-Q spectrogram is given by

$$X[k] = \frac{1}{N[k]} \sum_{n=0}^{N[k]-1} W[k,n]x[n]e^{-j2\pi Qn/N[k]} \tag{4}$$

where x is the digitized signal, $N[k]$ is the number of samples used to evaluate the expression for frequency sample k, $W[k,n]$ is a window function set to a Hanning window, for example, and Q is defined as $f/\Delta f$, where f is the frequency.

In the constant-Q spectrogram, cross-terms are reduced to zero unless the signal components overlap in time, as for the conventional spectrogram. However, there remains a tradeoff between time and frequency resolution that is based on the window length, which is quantified by a single value, the length of the window in terms of number of cycles.

Wigner Distribution

The Wigner distribution produces a time-frequency representation with the greatest resolution, but the representation also has very high cross-terms. The distribution is real, but it is not necessarily zero when the signal is zero, due to the cross-terms. It is zero before the signal starts and after the signal finishes, and it can have negative values.

The discrete Wigner distribution is given by

$$D(n,k) = \frac{1}{\pi} \sum_{-L+1}^{L-1} s^*(n-\tau) e^{-j4\pi k\tau/N} s(n+\tau) \tag{5}$$

where *s(n)* is the digitized signal and the limits on τ are included for practical evaluation of the sum. The total length, *2L-1*, should be equal to or longer than the duration of the signal.

The Wigner distribution is periodic with a period π. Therefore, to produce a representation that is free from aliasing, the signal must either be oversampled by a factor of two, or the analytic signal must be used. Using the analytic signal is preferable because it will reduce the number of cross-terms. Cross-terms appear when two frequency components interfere with each other, including interference between positive and negative frequencies. With the analytic signal, negative frequency components are no longer present.

Smoothed Pseudo-Wigner Distribution

The smoothed pseudo-Wigner distribution (SPWD) is an attempt to reduce the oscillating cross-terms in the Wigner distribution. Smoothing is applied independently in the time and frequency directions; therefore, there is no undesirable connection between the two resolutions as with the spectrogram. Smoothing degrades the resolution in the direction in which it is applied.

The SPWD is a filtered version of the Wigner distribution,

$$D(t,\omega) = \int L(t-t',\omega-\omega') D^{Wigner}(t',\omega') dt' d\omega' \tag{6}$$

where in our case, L is a Gaussian filter in each direction, $L(t,\omega)=(1/\alpha\beta)exp(-t\hat{}2/\alpha-\omega\hat{}2/\beta)$.

Choi-Williams Distribution

The Choi-Williams distribution was created to reduce cross-terms while preserving other desirable properties. The discrete version of the Choi-Williams distribution is given by Equation (20) of [6].

$$D(n,k) = 2 \sum_{\tau=-\infty}^{\infty} W_N(\tau) e^{-j2\pi k\tau/N} \times$$
$$\sum_{\mu=-\infty}^{\infty} W_M(\mu) \frac{1}{\sqrt{4\tau^2/\sigma}} \exp\left(-\frac{\mu^2}{4\tau^2/\sigma}\right) s(n+\mu+\tau) s^*(n+\mu-\tau) \tag{7}$$

where $W_N(t)$ is a symmetric window that is nonzero in the range, $t \in [-N/2, N/2]$, and $W_M(t)$ is a rectangular window that is nonzero in the range, $t \in [-M/2, M/2]$, effectively reducing the limits on the sums. σ is the parameter used to control the properties of the distribution. Large σ implies more smoothing and reduction of the cross-terms. However, this also leads to greater loss of resolution. The loss of resolution is not independently controlled for the time

and frequency directions because only one parameter is used. The Choi-Williams distribution also has the drawback that it is difficult to reduce cross-terms if two signal components occur at the same time or the same frequency [9].

TEST SIGNAL AND BASIS FOR COMPARISON

The operation of the linear amplitude-steered array has been simulated using the Field II program, developed by J. A. Jensen [10], [11]. The test signal is a simulated reflection from a set of seven point targets received by the amplitude-steered array operated in pulse-echo mode. The point targets are located at (6°, 4.0 m), (9°, 4.01 m), (12°, 4.02 m), (15°, 4.03 m), (18°, 4.04 m), (21°, 4.05 m), and (24°, 4.06 m). The amplitude weighting is determined so that the main beam is steered to 5° at 5.6 MHz. The transmitted signal is a linear FM chirp with frequency swept from 1.2 MHz to 5.6 MHz. The speed of sound is assumed to be 1500 m/s and, attenuation is not included. The transducer we simulate has a low-Q impulse response. The main effect of the transducer's transfer function is to reduce the amplitude of targets away from the resonance frequency of the transducer, not to effect resolution. Therefore, we replace the transducer's impulse response with an impulse.

The resolution of different distributions is measured as the -6-dB axial and lateral widths of each point target. The highest level of a cross-term relative to the maximum target amplitude in the image is also observed. Each distribution is optimized within the limits of the parameters available so that the axial and lateral resolutions of the point target at 6° are approximately equal and close to 1 cm and so that the highest level of a cross-term is at least 20 dB below the peak target. The criterion for highest level of a cross-term was chosen based on the appearance of the images. Lowering cross-terms causes a blurring of auto-terms. In most cases we do not have the degrees of freedom to control all of these criteria, so subjective evaluation is used to produce the best image.

RESULTS

The respresentations of the signal on the time-frequency plane are taken as images of a target. In the cases where the distribution has negative values, the absolute value is taken before logarithmic compression and display of the images.

Measured lateral and axial widths are presented in Table 1 and Table 2. Because of the high cross-terms for the Wigner distribution, measurements for targets at 12° to 21° are made using images with only a single target present at a time. The target at 24° was not measured because it appeared at the edge of the image. The target at 24° was not measured for the Choi-Williams distribution because it was not visible above the noise in the image.

The images produced with the spectrogram and constant-Q distributions are shown in Figure 2 and Figure 3. As expected, the spectrogram and constant-Q distributions did not have any cross-terms. The constant-Q distribution achieved better lateral resolution than the spectrogram, although the spectrogram generally produced better axial resolution. The constant-Q distribution maintained equal lateral and axial resolution for each individual target, while the spectrogram produced much better axial resolution than lateral resolution for the targets at lower frequencies.

An image formed using the Wigner distribution is shown in Figure 4. The Wigner distribution has no parameters for smoothing, and therefore the level of the cross-terms could not be reduced. In the image, only the targets at 6 and 9 degrees could be distinguished from the cross-terms. The Wigner distribution is still of interest as a measure of the achievable resolution.

Table 1. Measured lateral widths of the point spread function in mm.

Angle (deg)	6	9	12	15	18	21	24
Spectrogram	11.8	19.5	30.6	45.7	66.1	81.8	102
Constant-Q	11.1	17.2	23.2	31.0	37.6	42.6	48.7
Wigner[a]	11.1	16.6	21.5	28.4	34.7	38.5	--
SPWD	11.6	17.1	22.9	30.9	38.9	45.8	53.9
Choi-Williams	16.8	24.9	34.8	51.6	88.9	87.1	--

[a]Values for Wigner distribution were measured using images with one target present at a time.

Table 2. Measured axial widths of the point spread function in mm.

Angle (deg)	6	9	12	15	18	21	24
Spectrogram	11.2	11.2	14.9	16.8	18.7	18.7	24.3
Constant-Q	11.0	18.3	23.8	29.3	34.8	40.3	45.8
Wigner[a]	4.76	8.02	10.2	12.7	14.4	17.7	--
SPWD	7.07	9.41	12.2	14.1	16.0	19.0	21.4
Choi-Williams	7.10	9.89	13.0	14.8	15.6	20.6	--

[a]Values for Wigner distribution were measured using images with one target present at a time.

The smoothed pseudo-Wigner distribution, shown in Figure 5, performed the best of the distributions compared here in terms of combined lateral and axial resolution. Both lateral and axial resolutions were comparable to those for the Wigner distribution. And the cross-terms were reduced to 30 dB below the peak target signal.

The Choi-Williams distribution, shown in Figure 6, was not able to match the performance of the smoothed pseudo-Wigner distribution. As mentioned previously, cross-terms are difficult to suppress if signal components overlap in time or frequency. In our case, the two targets at the lower frequencies overlap enough in time and frequency that the cross-term between them could only be lowered below 20 dB at the cost of great loss in resolution. Therefore, some of the cross-terms were allowed to remain in the image at higher levels. Still, with only one parameter to control time and frequency smoothing and to control the cross-terms, we were unable to effectively trade more axial resolution for better lateral resolution.

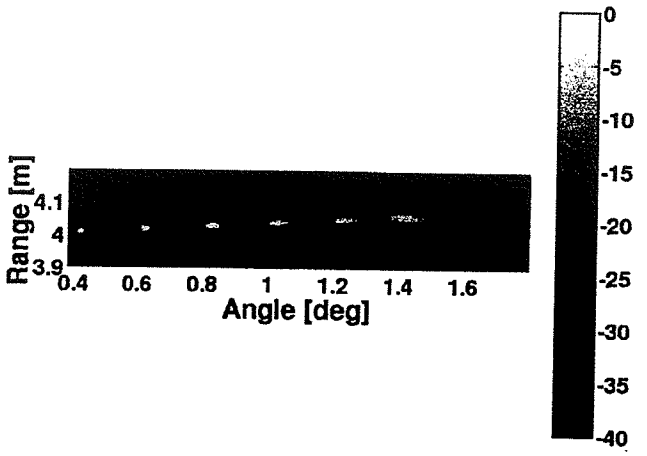

Figure 2. Image produced using the spectrogram. A 590-point (28.8 μs) Hanning window was used for the calculation.

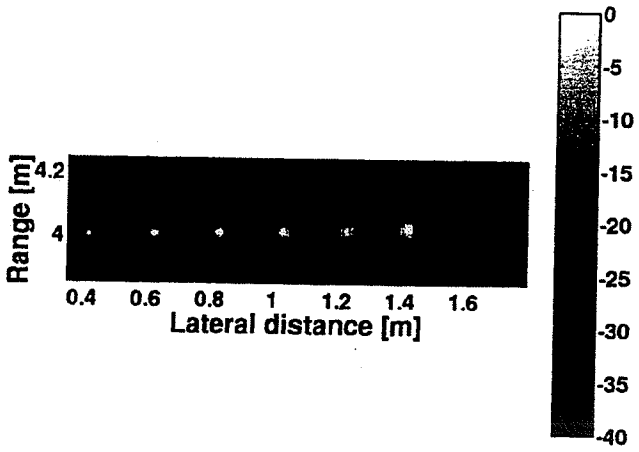

Figure 3. Image produced using the constant-Q spectrogram. The processing window contained 141 cycles (Q=141).

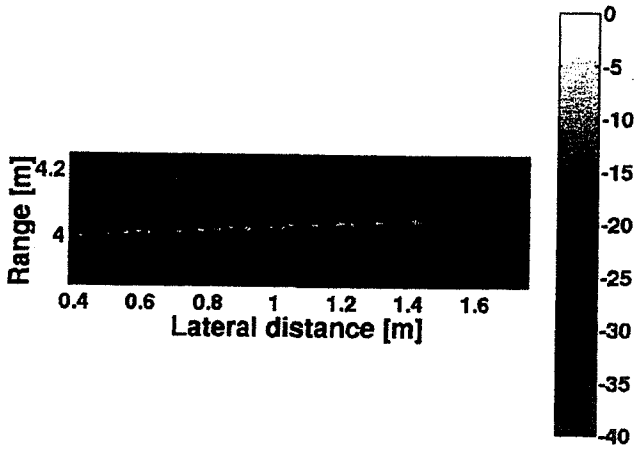

Figure 4. Image produced using the Wigner distribution. There were no parameters available for optimization.

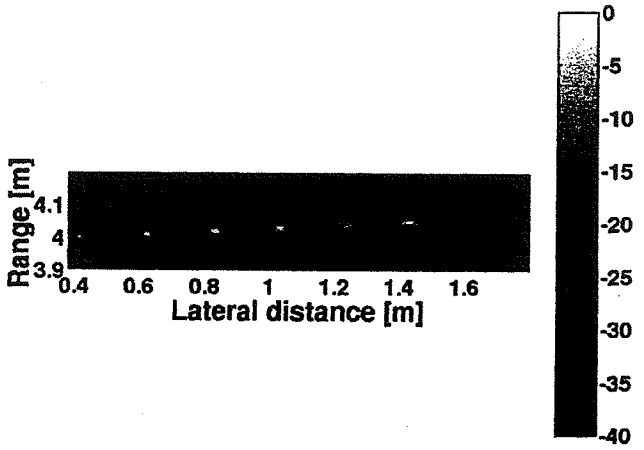

Figure 5. Image produced using the smoothed pseudo-Wigner distribution. The filter was Gaussian in both time and frequency directions. α=11.4E-12 s^2 and β=15.8E9 (rad/s)^2.

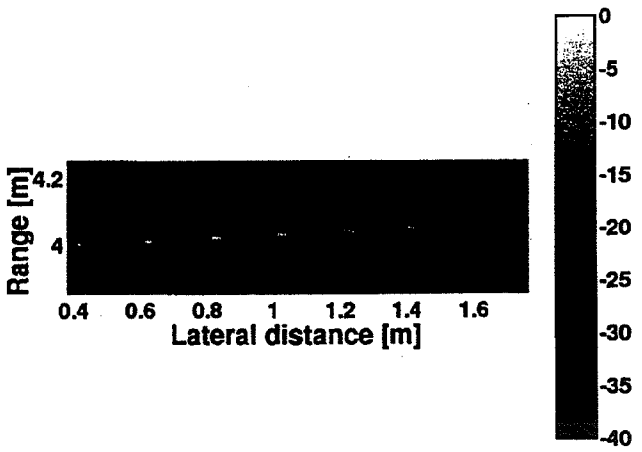

Figure 6. Image produced using the Choi-Williams distribution. W_M was a rectangular window with 256 points. W_N was a rectangular window with 513 points. σ was set to 0.75.

CONCLUSIONS

The performance of several time-frequency distributions were compared using a test signal, which represented a pulse-echo signal from seven point targets. By moving from the spectrogram to other time-frequency distributions, we have shifted from a tradeoff in axial and lateral resolution to a tradeoff in axial resolution, lateral resolution, and cross-term level. The smoothed pseudo-Wigner distribution gave the best overall results most likely because it has the most available parameters. Cross-terms were present at low levels. Axial and lateral resolutions approached those of the Wigner distribution.

REFERENCES

1. W. J. Hughes and W. Thompson, Jr., Tilted directional response patterns formed by amplitude weighting and a single 90° phase shift, *J. Acoust. Soc. Am.* **59**(5), 1040-1045 (1976).
2. C. H. Frazier, W. J. Hughes, and W. D. O'Brien, Jr., Analysis of resolution for an amplitude-steered array, *J. Acoust. Soc. Am.*, accepted (2000).
3. J. C. Brown, Calculation of a constant-Q spectral transform, *J. Acoust. Soc. Am.* **89**(1), 425-434 (1991).
4. T. A. C. M. Claasen and W. F. G. Mecklenbrauker, The Wigner distribution – A tool for time-frequency signal analysis, *Philips J. Res.* **35**(4/5) 276-300 (1980).
5. L. Cohen, Time-frequency distributions – A review, *Proc. of the IEEE* **77**(7), 941-981, (1989).
6. H.-I. Choi and W. J. Williams, Improved time-frequency representation of multicomponent signals using exponential kernels, *IEEE Trans. Acoust. Speech Sig. Proc.* **37**(6), 862-971 (1989).
7. P. Chevret, N. Gache, and V. Zimpfer, Time-frequency filters for target classification, *J. Acoust. Soc. Am.* **106**(4), 1829-1837 (1999).
8. L. R. Dragonette, D. M. Drumheller, C. F. Gaumond, D. H. Hughes, B. T. O'Connor, N.-C. Yen, and T. J. Yoder, The application of two-dimensional signal transformations to the analysis and synthesis of structural excitations observed in acoustical scattering, *Proc. of the IEEE* **84**(9), 1249-1263 (1996).
9. F. Hlawatsch and G. F. Boudreaux-Bartels, Linear and quadratic time-frequency representations, *IEEE Sig. Proc. Mag.* **9**, 21-67, 1992.
10. J. A. Jensen, FIELD: A program for simulating ultrasound systems, *Med. Biol. Engr. Comp.* **34** (1, Suppl.1), 351-353 (1996).
11. FIELD II program is available at the web site http://www.it.dtu.dk/~jaj/field/field.html.